Indian Journal of Novel Drug Delivery

IJNDD

An Official Publication of Karnataka Education and Scientific Society

Research Article

Sophora alopecuroides l. Total Alkaloids Loaded Magnetic/ph Sensitive Alginate-Chitosan Beads: Preparation and Physicochemical Characterization

YUAN-MEI HUANG [1], PING LI [1, 2*], YU-MIN LI [1, 2], AI-QIN WANG [3]

[1] Lanzhou University Second Hospital, Lanzhou, China

[2] Key Laboratory of Digestive System Tumors, Gansu Province, Lanzhou, China

[3] Lanzhou Institute of Chemical Physics, Chinese Academy of Sciences, Lanzhou, China

ARTICLE DETAILS

Article history:
Received on 25 February 2014
Modified on 28 June 2014
Accepted on 07 July 2014

Keywords:
Sophora alopecuroides L. total alkaloids,
Magnetic/pH sensitivity,
Hydrogel beads,
Swelling characteristic,
Delivery property

ABSTRACT

The aim of the present study was to prepare magnetic/pH sensitive alginate-chitosan beads loaded with the water-soluble traditional Chinese medicine *Sophora alopecuroides* L. total alkaloids by the ionic gelation method. Beads formulations based on the electrostatic interactions between alginate and chitosan were prepared via single factor design experiments, which were employed to investigate the combined effect of seven formulation variables, i.e., % of alginate, Fe_3O_4 nanoparticles to polymer, $CaCl_2$ and chitosan and the volume ratio of alginate to $CaCl_2$ and the crosslinking time and the polymer to drug on beads encapsulation efficiency and loading efficiency, considered as the responses to be optimized. Then, we characterized the optimal beads using SEM, FTIRS, XRD, and VSM, respectively, and investigated the influence of the swelling characteristic on the multifactorial relationships among formulation parameters. Furthermore, the delivery behavior of SATA from the optimal dry beads was evaluated in vitro. We found that the beads exhibited good pH-sensitive swelling, magnetic-response and controlled release properties due to their electrostatic interaction. The results together demonstrated that the beads can realize the goal of magnetic-target and have the potential to be used as a vehicle of SATA in the gastrointestinal administration.

INTRODUCTION

Recently, magnetic materials, which can be guided and aggregated more conveniently, had been used as drug carriers to manifest targeted delivery. And the iron sesquioxide or ferroso-ferric oxide nanoparticles is outstanding due to the exhibition of super-small mean diameter approximation, higher magnetization and excellent biocompatibility [1]. With the development of physical and pharmaceutical technology, many magnetic materials have been used in pharmaceutical preparation, for instance, magnetic liposome [2], magnetic microsphere [3], magnetic hydrogel [4], and so on. These dosage forms are mostly based on super- paramagnetic Fe_3O_4 nanoparticles, which could arrive exactly at the targeted tissue, then stay there with the help of physical force arising from the magnetic field (MF) and deliver the loaded drugs [5].

Author for Correspondence:
Email: gsliping@163.com

However, because of the fact that the magnetic nanoparticles are most likely to be rapidly erased by macrophages or the reticuloendothelial system before they arrive at the desired sites [6], it is vital to find methods to avoid this drawback. Fortunately, as environment-friendly materials, both alginate(Alg) and chitosan(CS), which can encapsulate efficiently the magnetic core and can be as a biodegradable polymer shell, have so much versatile biological activities, such as nontoxicity, superior biocompatibility and admirable biodegradability with ecological safety, that they are suitable to be utilized in biomedical and pharmaceutical formulations. There are several reports on Alg-CS based magnetic materials [7, 8], nonetheless, the preparation of magnetic polysaccharide beads is still deserve further studies.

Alg-CS gel has been drawn much more attention, oweing to its extensive usage in biotechnology and pharmaceutical industry for controlled drug

delivery [9-11]. Alginate is a natural linear biopolymer extracted from brown algae, which contains varying amounts of 1,4-linked β-D-mannuronicacid (M) and α-L-guluronicacid residues (G), and is composed of homo-polymeric blocks of M-M, G-G and M-G [12, 13]. On the one hand, sodium alginate has a unique property of crosslinking in the presence of multivalent cations, such as Ca^{2+}, Ba^{2+}, Sr^{2+} in aqueous media [14]; On the other hand, it can form the "egg-box" junctions polyelectrolyte complex induced by the strong electrostatic interaction between the amino groups of the chitosan and the carboxylic groups of the alginate [15].

Meanwhile, chitosan is a linear copolymer polysaccharide composed of D-glucosamine and N-acetyl-D-glucosamine units, which is soluble in acidic solvents and generally produced commercially by deacetylation of chitin, displaying its pH-response property in the application of stimulus-responsive hydrogels [16, 17]. In the Alg-CS beads, chitosan is used either as a mean of coating alginate beads to alter the diffusion rate of the encapsulated substances or as an additive to modify the beads structure [18-20]. Hence, they are pH sensitive materials and can be served as drug carries because of the amino groups in the chitosan molecule and carboxyl groups in the alginate molecule, which had already been used in controlled drug delivery technology for the gastrointestinal administration [21, 22].

Although many efforts had been given on investigating drugs using natural polymeric carriers, little had been given on the study of the water-soluble drugs. *Sophora alopecuroides* L. (*Leguminosae, Sophora Linn*. Chinese name "Kudouzi"), a useful traditional Chinese drug, is widely distributed in the Asian continent, especially in the northwest of China. This medicine is known to contain quinolizidine alkaloids as its principal bioactive constituents, which have been performed in terms of potential sedative, depressant, analgesic, hypothermic, antipyretic, cardiotonic activities, anti-tumor, and many other pharmacological activities [23, 24]. Phytochemistry investigations had showed that *Sophora alopecuroides* L. total alkaloids (SATA) contains more than twenty alkaloids, such as matrine, oxymatrine, sophoridine, sophocarpine, lehmannine, et al [25]. Many studies have been done on the detailed pharmacological mechanism of quinolizidine alkaloids, especially in the aspect of anticancer. It has been reported that quinolizidine alkaloids play an important effect on human tumor cells, including the inhibitory roles of growth, proliferation and induction of apoptosis, the changes of cell cycle, etc [26, 27]. Furthermore, the traditional Chinese drug SATA has the advantage of low-toxicity, which had made it become a new research theme in the anticancer's therapy. However, SATA is a strongly water-soluble drug with a low bioavailability after oral administration. Thus, SATA is certain significantly loaded in a magnetic/pH sensitive Alg-CS beads to expect to realize the goal of target localization, based on which beads would be efficiently centralized on the diseased region through the external MF after oral route. Then SATA could release from the beads for treatment of gastroenteric tumor.

Based on our previous works on a series of agents comprising lipophilic and water-soluble drug loaded in magnetic/pH sensitive beads, which was prepared through a two-step synthetic method loading the lipophilic drug [28] and loading a matrine monomer alkaloid [29], we pay attention on one-step crosslinking method which forms the Alg-CS beads and try to combine the water-soluble SATA, which may have more effect on cancer and possess more medicinal properties compared with the matrine monomer alkaloid. The goal is to enrich the employment of magnetic/pH sensitive drug delivery system in the treatment of gastrointestinal cancer.

In this study, we investigated a method of prepareing the beads by dropping alginate solution containing super-paramagnetic Fe_3O_4 nanoparticles and SATA into $CaCl_2$/CS solution, in which the process is mild and simple. Then, it was studied that various factors influence on the swelling characteristic of the optimal dry beads. In addition, the morphology, X-ray diffractometry, infrared spectrum, magnetic property, release behaviors were also studied. Lastly, the results were analyzed using a semi-empirical equation to reveal the drug release mechanism.

MATERIALS AND METHODS

Materials

CS (MW is 6.0×10^5, degree of deacetylation is 87%) was acquired from Lanzhou Institute of Chemical Physics, Chinese Academy of Sciences (Lanzhou, China). alginate of low viscosity (0.02 Pa·S) for a 1% solution at 20°C was purchased from Shanghai Chemical Co. Ltd (China), Fe_3O_4 (average size is 20 nm) was purchased from Nanjing Emperor Nano Material Co., Ltd

(Nanjing, China). SATA (purity 95.3%) was purchased from Ningxia Yanchi Zijinghua Medicine Industry Co., Ltd (Ningxia, China). All the other chemicals and reagents used were of analytical grade.

Single factor design experiments

Magnetic/pH sensitive Alg-CS beads were prepared based on the single factor design. The independent variables are Alg concentration, the weight ratio of Fe_3O_4 nanoparticles to Alg, $CaCl_2$ concentration, CS concentration, the volume ratio of Alg to $CaCl_2$, crosslinking time, and the weight ratio of polymer to drug. Furthermore, the encapsulation efficiency and loading efficiency were comprehensively considered as the evaluation parameters.

Preparation of the magnetic/pH sensitive Alg-CS beads loaded SATA

Alginate solution (w/v) was prepared by dissolving sodium alginate in deionized water. The mixed gelling medium was prepared as follows: chitosan was dissolved in 1% glacial acetic acid solution, which contains anhydrous calcium chloride. The magnetic/pH sensitive Alg-CS beads were prepared by ionic polymerization according to the following steps: SATA and Fe_3O_4 nanoparticles were mixed with 10ml prepared aqueous Alg solution adequately and sonicated until a uniform suspension was obtained. Then, the suspension was dropped into the mixed gelling medium through a 0.45 mm syringe needle for 20 min under gentle magnetic stirring. The distance between the edge of the needle and the surface of the mixed gelling medium was 6 cm. A series of the beads with different composition were prepared as shown in Table 1. The beads were collected and subsequently dried in air overnight.

Table 1: Formulation of the magnetic/pH sensitive Alg-CS beads utilizing single factor design

Formulation	Xa	Xb	Xc	Xd	Xe	Xf	Xg	Encapsulation effiviency[%]	Loading efficiency[%]
A1	1.5	1:3	2.5	0.2	1:2	20	5:1	24.00	8.81
A2	2.0	1:3	2.5	0.2	1:2	20	5:1	25.76	9.84
A3	2.5	1:3	2.5	0.2	1:2	20	5:1	41.54	16.23
B1	2.5	1:5	2.5	0.2	1:2	20	5:1	37.69	16.23
B2	2.5	1:7	2.5	0.2	1:2	20	5:1	40.27	17.75
C1	2.5	1:7	3.5	0.2	1:2	20	5:1	30.24	14.49
C2	2.5	1:7	1.5	0.2	1:2	20	5:1	38.16	19.87
D1	2.5	1:7	1.5	0.3	1:2	20	5:1	25.92	12.07
D2	2.5	1:7	1.5	0.4	1:2	20	5:1	26.30	12.03
E1	2.5	1:7	1.5	0.2	1:3	20	5:1	22.90	11.01
E2	2.5	1:7	1.5	0.2	1:4	20	5:1	21.88	10.90
F1	2.5	1:7	1.5	0.2	1:2	30	5:1	23.70	9.95
F2	2.5	1:7	1.5	0.2	1:2	10	5:1	29.65	15.70
G1	2.5	1:7	1.5	0.2	1:2	20	6:1	33.67	21.31
G2	2.5	1:7	1.5	0.2	1:2	20	4:1	25.13	13.49

[a] Alginate concentration (%, w/v) [b] Weight ratio of Fe_3O_4 nanoparticles to alginate (w/w). [c] $CaCl_2$ concentration (%, w/v). [d] Chitosan concentration (%, w/v). [e] Volume ratio of alginate to $CaCl_2$ (v/v). [f] Crosslinking time (min). [g] Weight ratio of polymer to drug (w/w).

Scanning electron microscopy (SEM)

The microstructure and surface topography of the beads were evaluated by scanning electron microscopy (SEM). Micrographs of the samples were taken using a SEM (JEOL, JSM-6380LV, Akishima Tokyo, Japan). Prior to observation, randomly selected beads were mounted on aluminum stubs, using double-sided adhesive tape, then hydrogel samples were coated with gold and scanned at an accelerating voltage of 15 kV.

Fourier transformation infrared spectroscopy (FTIRS)

Individual beads were crushed with pestle in an agate mortar, the crushed material was mixed

with potassium bromide in 1:100 proportions. The FTIRS spectra over the wavelength range 4000-500 cm^{-1} were recorded using a FTIRS (Thermo Nicolet, NEXUS, TM, USA).

X-ray diffractometry (XRD)

The X-ray diffractogram of SATA, chitosan, sodium alginate, Fe_3O_4 nanoparticles, blank magnetic/pH sensitive Alg-CS beads and SATA-loaded magnetic/pH sensitive Alg-CS beads were measured by an X-ray diffractometer (X' Pert PRO, Panalytical, Holland). X-ray of 1.54056 Å wavelength was generated by a Cu K_α source. The angle of diffraction was varied from 2θ from 10° to 50° at a step size of 0.03°.

Magnetic property

A vibrating-sample magnetometer (VSM) (Lake Shore, 735 VSM, Model 7304, USA) was used at room temperature to characterize the magnetic properties of pure Fe_3O_4 nanoparticles and SATA-loaded magnetic/pH sensitive Alg-CS beads. Magnetic response property of the beads can be evaluated by given magnetic field of about 3200 Oe to determine magnetic response time of the beads.

Swelling study

Swelling characteristics were conducted using the optimal dry beads. Accurately weighed amounts of the dry beads (ranging from 20 to 25 mg) were immersed in 20 ml HCl solution (pH 1.5) and phosphate buffer solution (pH 6.8) was prepared according to the Chinese Pharmacopoeia 2010 at 37°C. The beads were separated from the swelling medium at fixed time intervals. Immediately, they were wiped gently with filter paper and then weighed using electronic microbalance. The dynamic weight change of the beads with respect to time was calculated according to the formula:

$$\text{Swelling ratio (SR)} = \frac{(W-W_0)}{W_0} \quad \ldots\ldots (1)$$

Where W is the weight of the beads in the swollen state and W_0 is the initial weight of the beads.

Determination of srug encapsulation efficiency and loading efficiency

After preparing the dry beads, 50 milligrams of sample was crushed thoroughly and transferred into a beaker, drugs was extracted from the beads with 50 ml methanol by ultrasound at 37°C for 1 h. After rinsing the beaker thoroughly, the whole mixture was transferred into 50 ml volumetric flask. Than adding methanol to metered volume, the resulting solution was filtrated finally. The amount of drugs entrapped into the beads was calculated by high performance liquid chromatography (HPLC) (Agilent 1200, United States) at a wavelength of 220 nm determining the filtrated, which was determined from calibration curves of matrine in the methanol medium A=4.3318C-1.3319 (r=0.9999). The drugs encapsulation efficiency and loading efficiency of dry beads were estimated according to the formula as follows. All samples were analyzed in triplicate.

$$\text{Encapsulation efficiency (\%)} = \frac{\text{amount of SATA entrapped into beads}}{\text{SATA initial amount}} \times 100 \quad \ldots.(2)$$

$$\text{Loading efficiency (\%)} = \frac{\text{amount of SATA entrapped into beads}}{\text{weight of drug-loaded dry beads}} \times 100 \quad \ldots.(3)$$

In vitro drug release

The drug release properties from the optimal dry beads were determined as follows: the accurately weighed 500 mg of sample was suspended in 300 ml solution, which maintained at 37 °C±0.5°C under 100 rpm. The dissolution medium were hydrochloric acid solution (pH 1.5) and phosphate buffer solution of various pH (5.0, 6.8, 7.4 and 8.0), that were prepared according to the Chinese Pharmacopoeia 2010. At predetermined time intervals, 1 ml solution was withdrawn and analyzed for matrine at λ_{max} value of 220 nm by HPLC. Dissolution medium was maintained at constant volume by replacing the samples with a fresh dissolution medium. The drug release percent was determined using equation (4). All samples were analyzed in triplicate.

$$\text{Drug release (\%)} = \frac{R_t}{L} \times 100 \quad (4)$$

Where L and R_t represent the initial amount of drug loaded and cumulative amount of drug released at time *t*.

Release kinetics

The mathematical models, Higuchi $M_t/M_\infty = k_1 t^{1/2}$ equations were fitted to individual dissolution data with linear regression by SPSS 11.0 for Windows [30]. The drug release mechanisms of hydrogel beads were described by a semiempirical equation.

Statistical analysis

Statistical analysis for the determination of differences in the swelling characteristics within groups was accomplished using one-way analysis of variance, performed with a statistical program (SPSS 11.0 for Windows). For all statistical calculations, the level of significance was set at 0.05.

RESULTS AND DISCUSSION

Morphology observation

Fig. 1 shows SEM micrographs of the beads [Fig. 1(a-d)]. In comparison with the size of the wet beads which was 3 mm approximately, dry beads were shrunk at about half and their diameter was found to be about 1 mm. The wet beads were spherical, smooth, and reddish-brown revealing that super-paramagnetic Fe_3O_4 nanoparticles were dispersed uniformly in the Alg-CS matrix. In contrast, the beads had a rough structure on surface and the volume decreased after drying in air resulting in an irregular shape. Detailed examination of the surface structure indicated cracks and severe wrinkles caused by partial collapsing of the polymer network during dehydration.

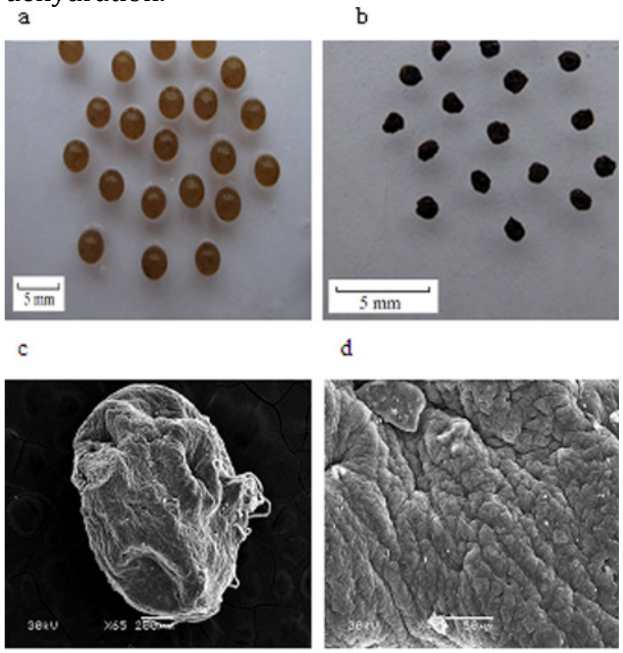

Figure 1: (a) Wet SATA-loaded magnetic/pH sensitive Alg-CS beads; (b) dry SATA-loaded magnetic/pH sensitive Alg-CS beads; SEM micrographs of surface morphology of dry SATA-loaded magnetic/pH sensitive Alg-CS beads: magnification (c ×65); (d ×400).

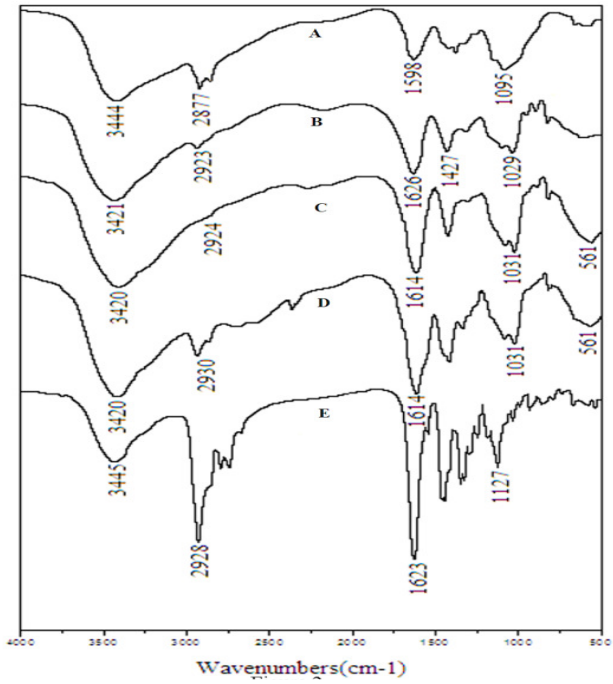

Figure 2: The FTIR spectra of chitosan(A), alginate(B), blank magnetic/pH sensitive Alg-CS beads(C), SATA-loaded magnetic/pH sensitive Alg-CS beads(D) and SATA(E).

It is well known that ionic cross-links will occur when alginate contacts with Ca^{2+} to form the "egg-box" structure. Furthermore, the formation of polyelectrolyte complex membrane via an ionic interaction between $-NH^{3+}$ of and $-COO^{-}$ groups of results in the formation of interpenetrating polymeric network. Therefore, in the preparation of the beads, Fe_3O_4 nanoparticles and drug were both encapsulated into the gel network composing the Alg and CS.

Fourier transformation infrared spectroscopy

The FTIR spectra of sodium alginate, chitosan, blank magnetic/pH sensitive Alg-CS beads, SATA-loaded magnetic/pH sensitive Alg-CS beads and SATA were shown in Fig. 2. The FTIR spectrum of CS showed a weak band of —OH stretching at 2877 cm^{-1} and the absorption band of the bending vibrations of the N-H (N-acetylated residues, amide II band) at 1598 cm^{-1}. The peaks observed at 1095 cm^{-1} were the secondary hydroxyl group (characteristic peak of —CH—OH in cyclic alcohols, C—O stretch). Sodium alginate showed the following distinct peaks: (1) strong absorption bands at 1626 and 1427cm^{-1} due to carboxyl anions (asymmetric and symmetric stretching vibrations); (2) The bridge oxygen (C—O—C, cyclic ether) stretching bands at 1029 cm^{-1}. For the blank beads, the

peaks observed at 1614, 1416, 1086, and 1031 cm^{-1} were the characteristic absorption band of CS and Alg. The absorption band at 1598 cm^{-1} of chitosan shifts to 1614 cm^{-1} after the reaction with alginate and the stretching vibration of —OH and —NH_2 at 3444 cm^{-1} shifts to 3420 cm^{-1} and comes broad, indicating that the polyelectrolyte complexes are formed and enhanced between chitosan and alginate. The characteristic absorption peak of Fe_3O_4 nanoparticles also appears at round 561 cm^{-1}.

It was obvious that the blank beads and the SATA-loaded beads indicated no distinct IR spectra. Apparently, the peaks at 3420 cm^{-1}(due to Alg-CS beads ν_{-OH} or ν_{-NH}) and 1624 cm^{-1} (due to SATA $\nu_{N-C=O}$) were found in the spectrum of the blank beads and SATA, respectively. However, in the spectrum of the SATA-loaded beads, the characteristic absorption peaks of SATA were almost masked by that of gel beads at 1614 cm^{-1} ($\nu_{c=c}$). Moreover, no new peaks were observed in the complex. Embedding in the polymers' matrix may increase stretching barrier for SATA intramolecular bonds, so the characteristic SATA peaks could not be identified. In addition, X-ray study confirmed SATA stability and its embedding in the beads at a molecular level.

X-ray diffraction

The X-ray diffraction patterns of the samples were presented in Fig. 3. The raw chitosan showed a broad prominence around 20° related to the anhydrous crystals. Meanwhile, the diffraction of alginate showed typical peaks around 19°, 28°, 29.5°, 32.5° and 34.5°. In contrast, Fig. 3 e) displayed that the characteristic diffraction peaks of chitosan and alginate all disappeared in the beads, suggesting that intermolecular interaction in this two compounds destroyed hydrogen bonding between amino groups and hydroxyl groups in chitosan [31]. In addition, some distinct peaks at 2θ values of 35.9°, 43.45°are assigned to the planes of Fe_3O_4 nanoparticles [32]. Therefore, Fe_3O_4 nanoparticles were successfully synthesized in the matrixs of the Alg-CS.

The SATA extract diffraction pattern shown in Fig.3 (d) displayed partial sharp crystalline peaks, such as significant peaks about at 11°, 15° and 18.5°, which is the characteristic of molecules with some crystallinity. Compared with that of the loaded beads, the crystalline peaks of SATA were not obtained in the complex shown in Fig. 3 (f), which undoubtedly confirms that SATA does not recrystallize in the gel beads, but it is embedded in the polymeric matrix at a molecular level.

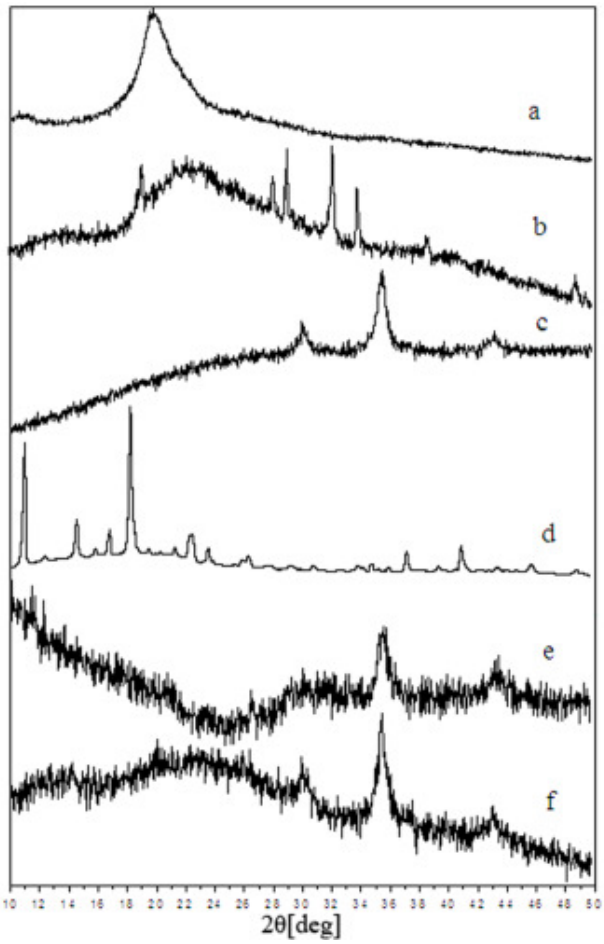

Figure 3: X-ray diffractograms of chitosan(a), alginate(b), Fe_3O_4 nanoparticles(c), SATA(d), blank magnetic/pH sensitive Alg-CS beads(e) and SATA-loaded magnetic/ pH sensitive Alg-CS beads(f).

Magnetic property

The magnetic properties of the dry beads are measured using a VSM. Fig. 4 exhibits the typical magnetization curve of pure Fe_3O_4 nanoparticles and SATA-loaded magnetic/pH sensitive Alg-CS beads. It can be seen that the saturation magnetization (σs) of the beads was about 5.02 emu/g, while the reference value for the pure magnetic Fe_3O_4 nanoparticles of σs was 58.81 emu/g. The reduced Ms (5.02 emu/g) can be attributed to the low content of Fe_3O_4 nanoparticles in the beads. Although the beads exhibit relatively low Ms, they show satisfactory magnetic-responsive aggregation and redispersion property in deionized water by adding or removing the MF. To say in other words, the dry beads possess satisfactory time-independent magnetic responsive ability and can be readily guided and collected together when

the external MF appears. As could be seen from Fig. 4, the hysteresis loop showed the super-paramagnetic property results from the magnetic Fe_3O_4 nanoparticles remained in these polymer beads.

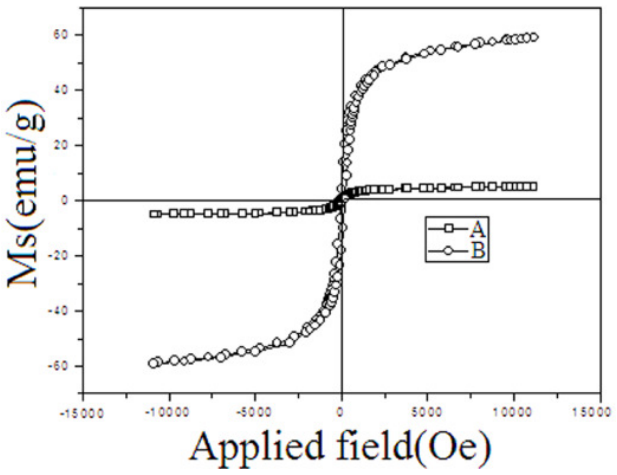

Figure 4: Magnetization curve of magnetic/pH sensitive Alg-CS beads: SATA-loaded magnetic/pH sensitive Alg-CS beads (A); pure Fe_3O_4 (B).

Swelling study

The swelling behavior of dry beads is mainly ascribed to the hydration of the hydrophilic groups of alginate and chitosan. The swelling ratio (SR) of magnetic/pH sensitive Alg-CS beads at pH 1.5 have no distinct difference among all the factors investigated ($p>0.05$). Thus, the figures of the SR of test beads at pH 1.5 were not shown.

1. Effect of Alg concentration on the swelling characteristic

Fig. 5 illustrates the swelling characteristic of magnetic/pH sensitive Alg-CS beads at various Alg concentrations. At pH 6.8, the SR of the test beads increased significantly compared with those at pH 1.5. As Alg concentration increased, the SR of test beads decreased and only a small difference in swelling was noticed ($p>0.05$). It was found that the beads (Alg concentration=2.5%) had a more spherical shape and smooth surface among all studied groups. Besides that, the low swelling ratio may retain drug better at the lower end of the gastric pH range.

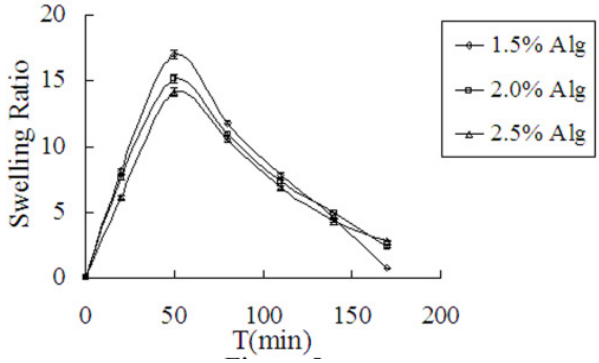

Figure 5: The influence of alginate concentration on the swelling characteristic from magnetic/pH sensitive Alg-CS beads (the weight ratio of Fe_3O_4 nanoparticles to Alg, 1/3; $CaCl_2$ concentration, 2.5%; CS concentration, 0.2%; the volume ratio of Alg to $CaCl_2$, 1/2; crosslinking time, 20 min; the weight ratio of polymer to drug, 1/5).

2. Effect of weight ratio of Fe_3O_4 nanoparticles to Alg on the swelling characteristic

Fig. 6 shows the effect of the weight ratio of Fe_3O_4 nanoparticles to Alg on the swelling characteristic. As shown, with increasing polymer weight, the SR of test beads increased significantly at pH 6.8. The two groups with the weight ratio of Fe_3O_4 nanoparticles to polymer of 1/5 and 1/7 showed no statistical difference ($p>0.05$), that are both appropriately taking into account magnetic responsivity. Among all the factors investigated, this factor could also affect the swelling characteristic at a great extent.

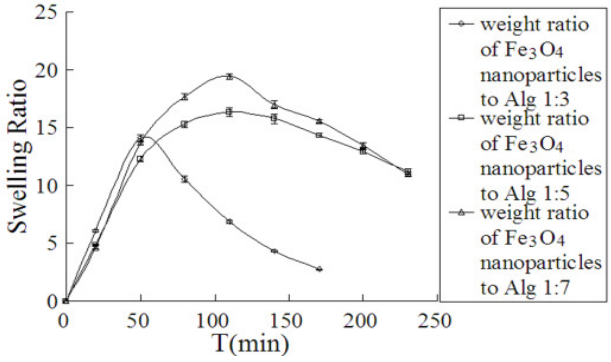

Figure 6: The influence of the weight ratio of Fe3O4 nanoparticles to Alg on the swelling characteristic from magnetic/pH sensitive Alg-CS beads (Alg concentration, 2.5%; CaCl2 concentration, 2.5%; CS concentration, 0.2%; the volume ratio of Alg to CaCl2, 1/2; crosslinking time, 20 min; the weight ratio of polymer to drug, 1/5).

3. Effect of $CaCl_2$ concentration on the swelling characteristic

Fig. 7 shows the swelling curves of magnetic/pH sensitive Alg-CS beads prepared at different concentration of $CaCl_2$. At pH 6.8, after decreasing the $CaCl_2$ concentration (from 2.5% to 1.5%), the crosslinking between Ca^{2+} and carboxylate ions became slower. Two groups of 2.0% and 2.5% $CaCl_2$ showed no statistical difference ($p>0.05$), The occurrence of higher SR is attributed to a larger swelling force created by the electrostatic repulsion between the ionized carboxyl groups. It appears that the less swelling of the beads is due to the higher crosslinking density of Ca^{2+} with carboxyl groups from Alg at higher $CaCl_2$.

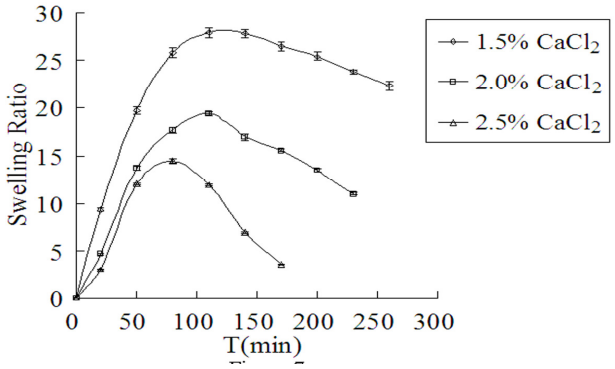

Figure 7: The influence of $CaCl_2$ concentration on the swelling characteristic from magnetic/pH sensitive Alg-CS beads (Alg concentration, 2.5%; the weight ratio of Fe_3O_4 nanoparticles to Alg, 1/7; CS concentration, 0.2%; the volume ratio of Alg to $CaCl_2$, 1/2; crosslinking time, 20 min; the weight ratio of polymer to drug, 1/5).

4. Effect of CS concentration on the swelling characteristic

Fig. 8 shows the effect of CS concentration on the swelling characteristic. As shown, with the increase of CS concentration, the SR of test beads decreased at pH6.8. It was detected that the maximum SR of the CS concentration (0.2%) was about 28.54 at pH 6.8, yet the maximum SR of the CS concentration (0.3% and 0.4%) were 18.93 and 17.92 respectively showing no statistical difference ($p>0.05$). Because the chitosan polymer network is physically entangled with the polymer chains of alginate, the dry beads possess greater swelling resistance when exposed to aqueous meida.

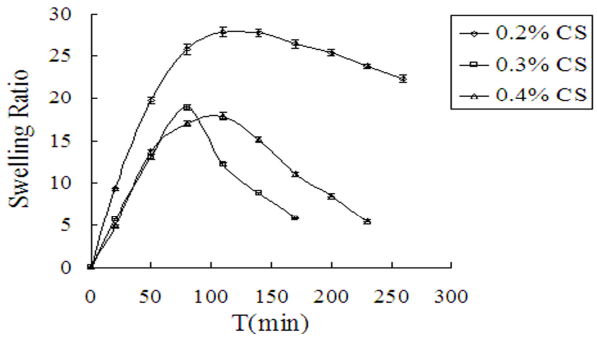

Figure 8: The influence of CS concentration on the swelling characteristic from magnetic/pH sensitive Alg-CS beads (Alg concentration, 2.5%; the weight ratio of Fe_3O_4 nanoparticles to Alg, 1/7; $CaCl_2$ concentration, 1.5%; the volume ratio of Alg to $CaCl_2$, 1/2; crosslinking time, 20 min; the weight ratio of polymer to drug, 1/5).

5. Effect of volume ratio of Alg to $CaCl_2$ on the swelling characteristic

Fig. 9 exhibits the influence of the volume ratio of Alg to $CaCl_2$ on the swelling characteristic. The SR of all test groups were approximately the same at pH 6.8 ($p>0.05$). Among all the factors investigated, the volume ratio of Alg to $CaCl_2$ had the least influence on the swelling characteristic. But, this factor has a great influence on the encapsulation efficiency and loaded efficiency of drug, which were decreased with increasing the volume ratio of Alg to $CaCl_2$. It was the main reason that SATA is a kind of hydrophilism substance, so the volume ratio of Alg to $CaCl_2$ was an important factor.

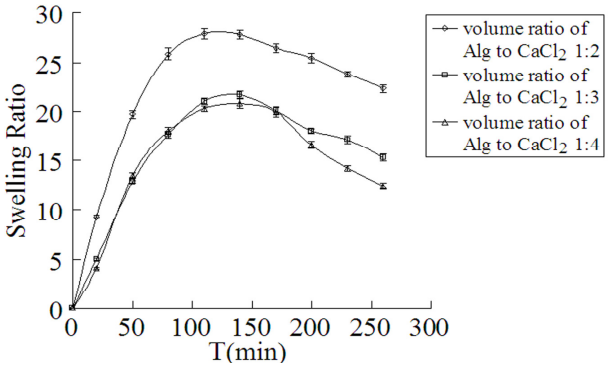

Figure 9: The influence of the volume ratio of Alg to $CaCl_2$ on the swelling characteristic from magnetic/pH sensitive Alg-CS beads (Alg concentration, 2.5%; the weight ratio of Fe_3O_4 nanoparticles to Alg, 1/7; $CaCl_2$ concentration, 1.5%; CS concentration, 0.2%; crosslinking time, 20 min; the weight ratio of polymer to drug, 1/5).

6. Effect of crosslinking time on the swelling characteristic

Fig. 10 shows the effect of crosslinking time on swelling characteristics of the dry beads. As can be seen, the SR of the test group with a crosslinking time of 30 min was lower than the other two groups at pH 6.8. The beads prepared in mixed gelling medium for 10 and 20 min showed faster swelling behavior than those of hydrogels prepared by the longer crosslinking time 30 min. Obviously, the longer crosslinking of the beads with Ca^{2+} is, the more structure of network becomes, because long crosslinking time might give a sufficient interacion time for the Alg-CS matrix. Therefore, the SR of test beads decreased significantly. However, taking into consideration of the facts that the encapsulation efficiency of drug at 30 min is lower than that at 20 min and the two groups with crosslinking time of 20 and 30 min showed no statistical difference ($p>0.05$). So we chose 20 min as crosslinking time.

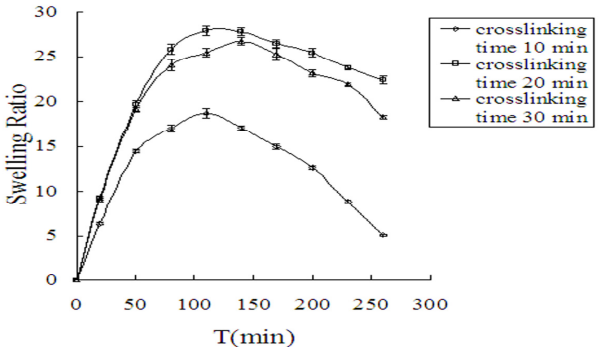

Figure 10: The influence of crosslinking time on the swelling characteristic from magnetic/pH sensitive Alg-CS beads (Alg concentration, 2.5%; the weight ratio of Fe_3O_4 nanoparticles to Alg, 1/7; $CaCl_2$ concentration, 1.5%; CS concentration, 0.2%; the volume ratio of Alg to $CaCl_2$, 1/2; the weight ratio of polymer to drug, 1/5).

7. Effect of weight ratio of polymer to drug on the swelling characteristic

The weight ratio of polymer to drug on the swelling characteristic is also an important factor influencing the swelling characteristic. As Fig. 11 shows, the SR of test beads with weight ratio of polymer to drug of 1/5 was higher than that of the other two groups at pH 6.8, in which weight ratios were approximately 1.09 at pH 1.5 and 28.54 at pH 6.8 ($p < 0.05$). Obviously, the higher the weight ratio of polymer to drug is, the higher the encapsulation efficiency becomes.

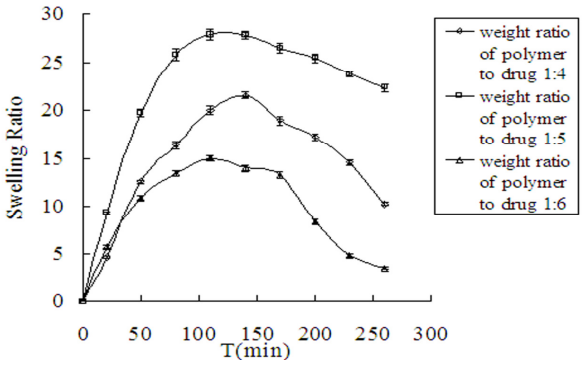

Figure 11: The influence of the weight ratio of polymer to drug on the swelling characteristic from magnetic/pH sensitive Alg-CS beads (Alg concentration, 2.5%; the weight ratio of Fe_3O_4 nanoparticles to Alg, 1/7; $CaCl_2$ concentration, 1.5%; CS concentration, 0.2%; the volume ratio of Alg to $CaCl_2$; 1/2; crosslinking time, 20min).

8. Swelling study in solutions of various pH

Fig. 12 illustrates the swelling behavior of dry beads that prepared by means of optimal composition of single factor design experiment in HCl solution (pH 1.5) and solutions phosphate buffer of various pH (5.0, 6.8, 7.4, 8.0). As can be seen, the test beads exhibited significant swelling ratio when exposed to the slightly alkaline environment. The SR at pH 6.8 was 28 times higher than that at pH 1.5. The swelling mechanism in slightly alkaline environment is related to the exchange of Ca^{2+} with Na^{+}, the lower binding of chitosan with alginate leading to less stable beads, and the ionization of carboxyl groups in neutral pH resulting in higher SR. Likewise, after swelling for 1-2 hours in solution of pH 6.8, 7.4, 8.0, the swelling ratio began to decline because of the disintegration of beads. In contrast, the test beads shrink in acidic conditions due to the fact that beads possess greater swelling resistance when exposed to aqueous media because of the greater physical entanglement of the polymer. Therefore, with the evolution of time, the SR of beads is not increased. To summarize, it is obvious that the swelling behavior of the beads manifests its pH sensitivity.

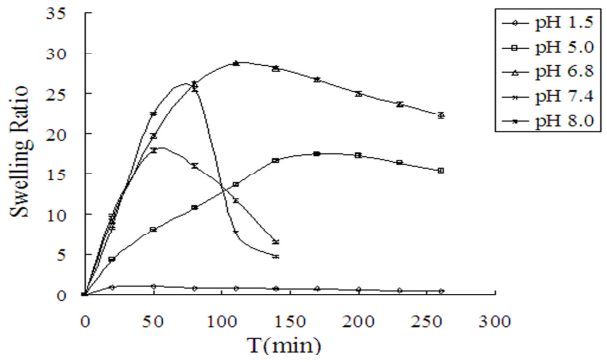

Figure 12: Swelling characteristics of SATA-loaded beads in HCl solution (pH 1.5) and different phosphate buffer solutions (pH 5.0, 6.8, 7.4 and 8.0).

Drug release study

Fig. 13 shows the cumulative release feature of SATA from the dry beads. SATA was released from Alg-CS in hydrochloric acid solution (pH 1.5) and other different phosphate buffer solutions (pH5.0, 6.8, 7.4, 8.0). As seen in fig. 13, when the release time was 2 h, the cumulative release was 49.17% at pH 1.5, 58.65% at pH5.0, 87.43% at pH 6.8, 86.44% at pH 7.4, 91.72% at pH 8.0, respectively. Time of about 95% SATA released from beads was 3.0 h at pH 6.8. However, when the release time was 12.0 h at pH 1.5, its cumulative release approached about 84.39%. Apparently, the beads were disintegrated at pH 6.8-8.0 so that dissolution of the drug from beads became more quickly than that at pH 1.5. This suggests that the water-soluble drug release properties of hydrogel beads are not chiefly concerned with the pH sensitive characterisation of beads swelling. This phenomenon maybe attributed to the fact that the drug exists in the polymeric matrix at molecule modality.

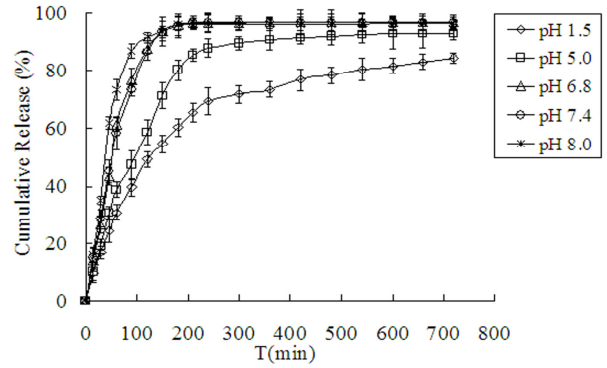

Figure 13: The cumulative release curves of SATA from magnetic/pH sensitive Alg-CS beads at various pH of media at 37 °C ± 0.5°C (pH 1.5, 5.0, 6.8, 7.4, 8.0).

Graphical abstract: SATA loaded magnetic/pH sensitive alginate-chitosan beads was prepared, then the physicochemical characterization, swelling study and drug delivery in vitro were also investigated.

Release kinetics

$$M_t/M_\infty = k_1 t^n \quad \text{or}$$
$$\text{Log}\,(M_t/M_\infty) = \log k_1 + n \log t \qquad (5)$$

Where M_t/M_∞ is the fractional amount of the drug released at time t, n is a diffusion exponent which indicates the release mechanism, and k_1 is a characteristic constant of the system. From the slope and intercept of the plot of $\log(M_t/M_\infty)$ versus log t, kinetic parameters n and k_1 were calculated. For spheres, values of n between 0.43 and 0.85 are indications of both diffusion controlled drug release and swelling controlled drug release (anomalous transport). Values above 0.85 indicate case-II transport which relates to polymer relaxation during gel swelling. Values below 0.43 indicate that drug release from polymer was due to Fickian diffusion [33].

The release rate constant was calculated by fitting the experimental drug release data into the dissolution models. And the goodness-of-fit of the drug release data was evaluated by linear regression. SATA release kinetics from magnetic/pH sensitive Alg-CS beads at different pH was shown in Table 2. After 2 hours, the remaining drug is released almost linearly at pH 6.8–8.0. At pH 1.5–5.0, the release was due to Anomalous transport, whereas, drug release mechanism at pH 6.8–8.0 was induced by Fickian diffusion.

Table 2: Estimated parameters and drug release mechanism of magnetic/pH sensitive Alg-CS beads at media of pH 1.5, 5.0, 6.8, 7.4 and 8.0. Kinetic constants, diffusional exponents, and correlation coefficients, by linear regression of $\log(M_t/M_\infty)$ vs. log t.

pH	n[a]	k[b]	r[c]	Drug Transport Mechanism
1.5	0.5233	0.15918	0.9388	Anomalous transport
5.0	0.5225	0.24502	0.9284	Anomalous transport
6.8	0.4072	1.50661	0.8252	Fickian Diffusion
7.4	0.3972	1.71751	0.8340	Fickian Diffusion
8.0	0.3343	4.14572	0.8101	Fickian Diffusion

[a]Diffusional exponents indicatives of the drug release mechanism. [b]Kinetic constants k is the constant related to the structural and geometric characteristic of the device. [c]Correlation coefficients.

CONCLUSIONS

In a conclusion, the magnetic/pH sensitive Alg-CS beads loading SATA, containing more than twenty effective alkaloids which could have positive effect on gastrointestinal tumor cell and possess good medicinal properties, was prepared by simple ionic gelation and novel nontoxic method. The results showed that the optimal beads were prepared at the Alg concentration 2.5%, the weight ratio of Fe_3O_4 nanoparticles to polymer 1/7, the $CaCl_2$ concentration 1.5%, the CS concentration 0.2%, the volume ratio of Alg to $CaCl_2$ 1/2, the crosslinking time 20 min, and the weight ratio of polymer to drug 1/5. This study showed the swelling characteristic and delivery behavior of SATA from the beads in vitro. Furthermore, the results reveal that usually the beads swelled and the drug was released quickly in alkaline conditions (such as in simulated intestinal fluid), while under acidic conditions (such as in simulated gastric fluid) they remained in a shrinkage state and the drug was released relatively slowly. In addition, the beads possess satisfactory time-independent magnetic responsive ability due to the fact that its saturation magnetization (σs) is about 5.02emu/g. The overall results indicate that the beads have potential to be used as a promising vehicle for SATA in the gastrointestinal administration and promote the development of magnetic/pH sensitive drug delivery system.

ACKNOWLEDGEMENTS

This study was supported by the Pedestal Plan Fund for Science and Technology of Gansu province, China (Grant No: 0708NKCA129).

DECLARATION OF INTEREST

The authors report no conflicts of interest. The authors alone are responsible for the content and writing of the paper.

REFERENCES

[1] J. Roger, J.N. Pons, Massart R, A. Halbreich, J.C. Bacri, Some biomedical applications of ferrofluids, Eur. Phys. J. AP. 5 (1999) 321-328.

[2] P. Pradhan, J. Giri, F. Rieken, C. Koch, O. Mykhaylyk, M. Döblinger, R. Banerjee, D. Bahadur, C. Plank, Targeted temperature sensitive magnetic liposomes for thermo-chemotherapy, J. Control. Release 142 (2010) 108-121.

[3] E. Ruiz-Hernández, A. López-Noriega, D. Arcos, M. Vallet-Regó, Mesoporous magnetic microspheres for drug targeting, Solid State Sci. 10 (2008) 421-426.

[4] A.T. Paulino, L.A. Belfiore, L.T. Kubota, E.C. Muniz, V.C. Almeida, E.B. Tambourgi, Effect of magnetite on the adsorption behavior of Pb(II), Cd(II), and Cu(II) in chitosan-based hydrogels, Desalination 275 (2011) 187-196.

[5] S. Kayal, R.V. Ramanujan, Doxorubicin loaded PVA coated iron oxide nanoparticles for targeted drug delivery, Mater. Sci. Eng., C 30 (2010) 484-490.

[6] A.K. Gupta, M. Gupta, Synthesis and surface engineering of iron oxide nanoparticles for biomedical applications, Biomaterials 26 (2005) 3995-4021.

[7] P.V. Finotelli, D.D. Silva, M. Sola-Penna, A.M. Rossi, M. Farina, L.R. Andrade, A.Y. Takeuchi, M.H. Rocha-Leão, Microcapsules of alginate/chitosan containing magnetic nanoparticles for controlled release of insulin, Colloids Sur., B 81 (2010) 206-211.

[8] H.J. Liu, P. Li, Q. Wei, Magnetic N-succinyl chitosan/alginate beads for carbamazepine delivery, Drug Dev. Ind. Pharm. 36 (2010) 1286-1294.

[9] W.R. Gombotz, S.F. Wee, Protein release from alginate matrices, Adv. Drug Deliv. Rev. 31 (1998) 267-285.

[10] Y.N. Dai, P. Li, J.P. Zhang, A.Q. Wang, Q. Wei, A Novel pH Sensitive N-Succinyl Chitosan/ Alginate Hydrogel Bead for Nifedipine Delivery, Biopharm. Drug Dispos. 29 (2008) 173–184.

[11] N. Mennini, S. Furlanetto, M. Cirri, P. Mura, Quality by design approach for developing chitosan- Ca-alginate microspheres for colon delivery of celecoxib-hydroxypropyl-b-cyclodextrin-PVP complex, Eur. J. Pharm. Biopharm. 80 (2012) 67-75.

[12] M. George, T.E. Abraham, Polyionic hydrocolloids for the intestinal delivery of protein drugs: Alginate and chitosan — a review, J. Control. Release 114 (2006) 1-14.

[13] L.W. Chan, H.Y. Lee, P.W.S Heng, Production of alginate microspheres by internal gelation using an emulsification method, Int. J. Pharm. 242 (2002) 259-262.

[14] B.T. Stokke, O. Smidsroed, P. Bruheim, G. Skjaak-Braek, Distribution of uronate residues in alginate chains in relation to alginate gelling properties, Macromolecules 24 (1991) 4637-4645.

[15] X.Z. Shu, K.J. Zhu, The influence of multivalent phosphate structure on the properties of ionically cross-linked

chitosan films for controlled drug release, Eur. J. Pharm. Biopharm. 54 (2002) 235-243.
[16] P. Baldrick. The safety of chitosan as a pharmaceutical excipient, Reg Toxicol Pharm 56 (2010) 290-299.
[17] O. Felt, P. Buri, R. Gurny, Chitosan: A Unique Polysaccharide for Drug Delivery, Drug Dev. Ind. Pharm. 24 (1998) 979-993.
[18] A.K. Anal, W.F. Stevens, Chitosan-alginate multilayer beads for controlled release of ampicillin, Int. J. Pharm. 290 (2005) 45-54.
[19] T. Gotoh, K. Matsushima, K.I. Kikuchi, Preparation of alginate-chitosan hydrogel beads and adsorption of divalent metalions, Chemosphere 55 (2004) 135-140.
[20] Y.H. Lin, H.F. Liang, C.K. Chung, M.C. Chen, H.W. Sung, Physically crosslinked alginate/ N, O-carboxymethyl chitosan hydrogels with calcium for oral delivery of protein drugs, Biomaterials 26 (2005) 2105-2113.
[21] T. Chandy, D.L. Mooradian, G.H.R Rao, Chitosan/polyethylene glycol–alginate microcapsules for oral delivery of hirudin, J. Appl. Polym. Sci. 70 (1998) 2143-2153.
[22] G. Pasparakis, N. Bouropoulos, Swelling studies and in vitro release of verpamil from calcium alginate and calcium alginate-chitosan beads, Int. J. Pharm. 323 (2006) 34-42.
[23] Atta-ur-Rahman, M.I. Choudhary, K. Parvez, A. Ahmed, F. Akhtar, M. Nur-e-Alam, N. M. Hassan, Quinolizidine Alkaloids from *Sophora alopecuroides*, J. Nat. Prod. 63 (2000) 190-192.
[24] H.Y. Gao, G.Y. Li, J.H. Wang, Studies on the dynamic accumulations of *Sophora alopecuroides L. Alkaloids* in different harvest times and the appropriate harvest time, J. Chromatogr. B 879 (2011) 1121-1125.
[25] Y.Q. Yu, P. Ding, D.F. Chen, Determination of quinolizidine alkaloids in Sophora medicinal plants by capillary electrophoresis, Anal. Chim. Acta 523 (2004) 15-20.
[26] G. Song, Q. Luo, Q. Jian, L. Wang, Y.S. Shi, C.X. Sun, Effects of oxymatrine on proliferation and apoptosis in human hepatoma cells, Colloids Sur., B 48 (2006) 1-5.
[27] Y.F. Zhang, S.Z. Wang, Y.Y. Li, Z.Y. Xiao, Z.L. Hu, J.P. Zhang, Sophocarpine and matrine inhibit the production of TNF-αand IL-6 in murine macrophages and prevent cachexia-related symptoms induced by colon26 adenocarcinoma in mice, Int. Immunopharmacology 8 (2008) 1767-1772.
[28] F.Q. Wang, P. Li, J.P. Zhang, A.Q. Wang, Q. Wei, pH-sensitive magnetic alginate-chitosan beads for albendazole delivery, Pharm. Dev. Techno. 16 (2011) 228-236.
[29] L.L. Zhang, P. Li, Y.M. Li, A.Q. Wang, Preparation and characterization of magnetic alginate-chitosan hydrogel beads loaded matrine, Drug Dev. Ind. Pharm. 2011 in press.
[30] M. Kılıc-arslan, T. Baykara, The effect of the drug/polymer ratio on the properties of the verapamil HCl loaded microspheres, Int. J. Pharm. 252 (2003) 99-109.
[31] J.H. Kim, Y.M. Lee, Synthesis and properties of diethylaminoethyl chitosan, Polymer 34 (1993) 1952-1957.
[32] K.R. Reddy, K.P. Lee, A.G. Iyengar, Synthesis and characterization of novel conducting composites of Fe_3O_4 nanoparticles and sulfonated polyanilines, J. Appl. Polym. Sci. 104 (2007) 4127-4134.
[33] F.N. Xi, J.M. Wu, Z.S. Jia, X.F. Lin, Preparation and characterization of trypsin immobilization on silica gel supported macroporous chitosan beads, Process Biochem. 40 (2005) 2833-2840.